

# A study of positional disorder in strontium barium niobate

M. P. TRUBELJA, E. RYBA\*, D. K. SMITH‡

*Mineral Processing Program, Department of Mineral Engineering, \*Department of Materials Science and Engineering, and ‡Departments of Materials Science and Engineering and Geosciences, The Pennsylvania State University, University Park, PA 16802, USA*

The first systematic examination of trends in the site occupancies of strontium and barium ions in strontium barium niobate (SBN) at three compositions across the phase range is presented. X-ray powder diffraction and Rietveld structure refinement were used to obtain refined structures for SBN. Some problems were encountered in the structure refinement due to the domain structure in the material. Barium was found only at the A2 site for each composition. Ba/Sr occupancy for the A2 site varied from 91% for SBN (72–28) to 99% for SBN (50–50) in the unannealed state, while strontium occupancy of the A1 site varied from 70% to 54%. In annealed SBN (50–50), the A2 site occupancy decreased to 95%, while the A1 site occupancy increased to 62%. It is proposed that a twisting of the structure in the unannealed state decreases the sizes of the cages at the A1, A2 and C sites. After annealing, the structure becomes more regular, enlarging the A1, A2 and C sites and allowing more strontium atoms to occupy the A1 site. Cation distribution is controlled by the twisting of the octahedral framework. The overall properties of the material are modified by this distortion of the structure.

## 1. Introduction

### 1.1. The tungsten bronze family

The tungsten bronze family is one of several structural families which yield ferroelectric materials. The tungsten bronze structure was deduced by Magneli [1] for the phase  $K_x\text{WO}_3$ . Since that time, numerous tungsten bronzes have been synthesized, many of which show strong ferroelectric behaviour. While tungsten bronzes can exhibit different symmetries and lattice types from monoclinic to cubic, two of the forms are most common. The first is orthorhombic, with space group  $Cmm2$ , having approximate lattice parameters  $a, b = 1.7 \text{ nm}$ ,  $c = 0.39 \text{ nm}$ . The second is tetragonal, with space group  $P4bm$  and approximate lattice parameters of  $a, b = 1.2 \text{ nm}$ ,  $c = 0.39 \text{ nm}$ .

The basic formula for a ferroelectric tetragonal tungsten bronze is  $(A_{1-x}, A_{2-2x}, C)\text{M}_2\text{O}_6$ . The skeletal framework of the tungsten bronze structure is formed by the  $\text{MO}_6$  octahedra (Fig. 1). These octahedra share corners to form the cavities around the A1, A2, and C sites (Figs 2 and 3) [2]. The octahedra in the structure contain two cation sites, M(1) and M(2). Four of the oxygen atoms surrounding each M cation are in the same  $z$  plane and form a quasi-square. Four O(1)s surround the M(1) cation in the oxygen sheet, while O(1), O(2) and O(3) atoms surround the M(2) cation in the oxygen sheet. Above and below the M(1) cation are the O(4a) or O(4b) sites, completing the octahedra (Fig. 1). O(5a) or O(5b) atoms finish the M(2) octahedra. There are two sets of positions for both the O(4) and O(5) atoms. These oxygen atoms, depending

upon the occupancy of the sites for the A1, A2, and C cations, often disorder or split in position to form a domain structure. M cations commonly found in tungsten bronzes are tantalum, niobium, tungsten and molybdenum atoms.

One of the three cation sites created by the octahedral framework, is the A1 site. Twelve oxygen atoms surround this site in a nearly cubo-octahedral arrangement (Fig. 2). Fig. 4 shows the placement of the A1 site within the tetragonal unit cell. The oxygen atoms which surround the A1 site are the O(2) and O(5a) or O(5b) atoms. The A2 site appears to lie in a distorted pentagonal channel. On closer examination, the A2 site reveals a tri-capped trigonal prismatic coordination. Tri-capped trigonal prismatic coordination can be thought of as a triangular channel consisting of nine atoms coordinated about the central cation. The grouping of the anions at the A2 site is two O(1) and one O(3) atoms, which form a triangle above the A2 cation, with another set of O(3) and O(1) atoms forming the base of the prism. At half height, in staggered positions to the O(1) and O(3) atoms, are the O(5a) or O(5b) atoms and the O(4a) or O(4b) atoms. Fig. 3 shows the coordination for the A2 site. When two A cations are found in the tungsten bronze structure, the smaller one is usually in the A1 site. This preference of the smaller cations for the A1 site has always been a paradox because, when the tungsten bronze structure was solved [2], the A1 site was identified as being larger than the A2 and C sites because of the higher coordination number (C.N.) (12 versus

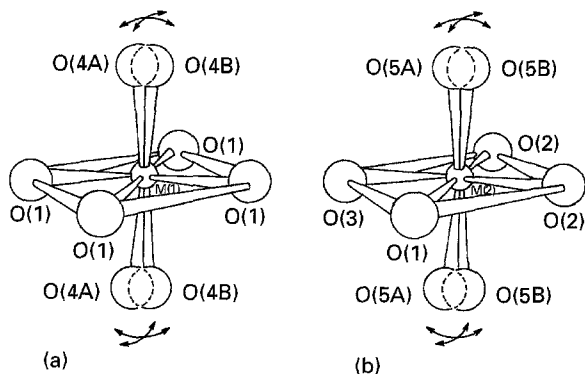


Figure 1 (a) M(1) and (b) M(2) octahedra for the tungsten bronze structure. After Jamieson *et al.* [2].

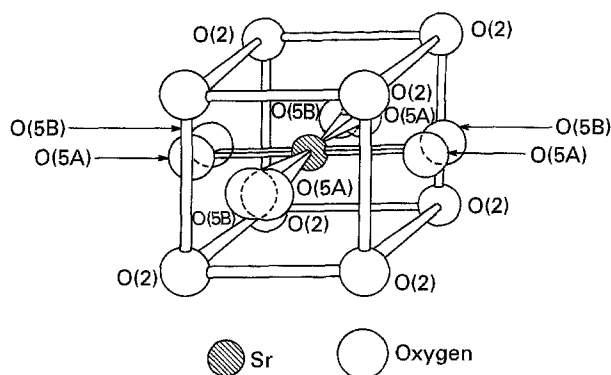


Figure 2 Cubo-octahedral coordination of the nearest neighbour oxygen atoms around strontium in the A1 site. After Jamieson *et al.* [2].

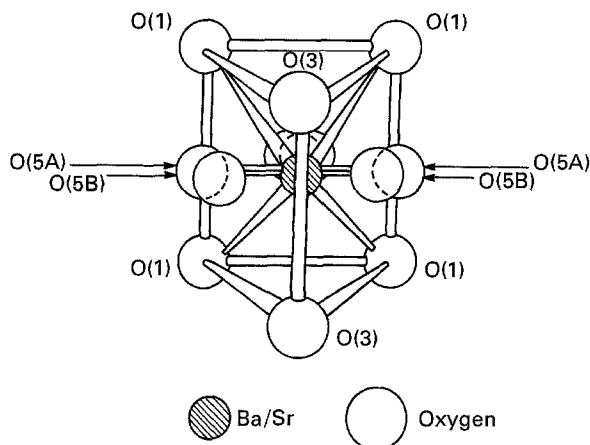
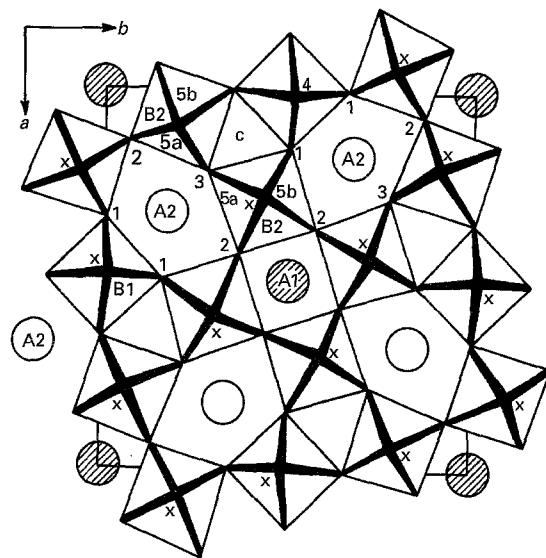


Figure 3 Tri-capped trigonal prismatic coordination of the nearest neighbour oxygen atoms around a composite Ba/Sr atom in the A2 and C sites. After Jamieson *et al.* [2].

9 for the A2 site). The A1 and A2 sites can accept a wide variety of A cations. Some of the common A cations are lead, barium, calcium, strontium, potassium, sodium and many of the rare-earth elements.

The C site (Fig. 4) is the smallest of the three cavities created by the framework of octahedra. The C site coordination also forms a tri-capped trigonal prism with nine coordination. The C cation is surrounded by two sets of O(1) and O(3) anions. These atoms form two triangles, one at the base and one at the top of the prism. In staggered positions, at half-height, forming



x, alternative oxygen site in niobium oxygen octahedra

Site preferred by Sr ( $z = 0.5$ )

Disordered site, Ba-Sr site ( $z = 0.5$ )

Figure 4 View of strontium barium niobate structure along the polar  $c$  axis. After Jamieson *et al.* [2].

a distorted triangle, are one O(4) and two O(5) atoms. The smallest cations in the structure are usually located at the C site. Cations which commonly occupy the C site are lithium, magnesium and beryllium.

There are several reasons why the tungsten bronze structure is so complicated. Each of the  $MO_6$  octahedra can tilt several degrees in various directions from the  $c$  axis, which shifts the apical O(4a), O(4b), O(5a), and O(5b) atoms. Jamieson *et al.* [2] proposed the idea that the tilting of the  $MO_6$  octahedra, when different types of A and C cations are added to the structure, causes the symmetry to change from tetragonal to orthorhombic. The atoms involved in these shifts are the O(9) and O(10) atoms which are located at the apex of the corner and edge octahedra of the orthorhombic cell for barium sodium niobate (70–30) and are equivalent to the O(4a) or O(4b) and O(5a) or O(5b) atoms in the tetragonal tungsten bronze cell. The positions of the O(9) and O(10) atoms are shown in Fig. 5. The second major reason this structure is so complex is that the O(4) site may have only 50% occupancy [2]. These vacancies cause other atoms to shift from their ideal positions and change the local site symmetries.

In order to have a ferroelectric material, it is necessary for some of the atoms to shift within the structure to create a dipole. For this structure, the atoms displaced are the cations in the M(1), M(2), A1, A2, and C (if present) sites. These atoms are offset from the O(1), O(2), and O(3) sheet oxygen atoms. This shift of the cations creates a number of dipoles oriented in the same direction (along the  $c$  axis), making it ferroelectric.

This family of compounds is useful for electronic materials because many of them have very high values for the dielectric constant and the pyroelectric and electro-optic coefficients. Many materials of this structure family are also relaxor ferroelectrics. Because

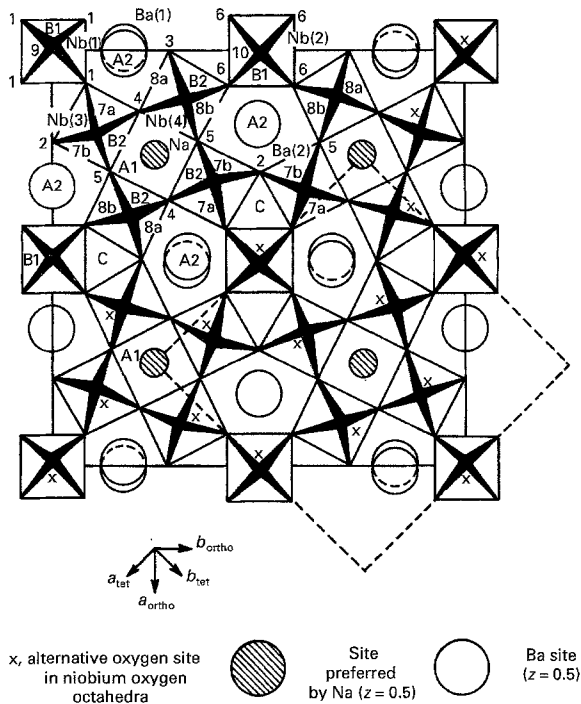


Figure 5 View of the orthorhombic barium sodium niobate structure BNN(70–30) along the polar  $c$  axis; the related tetragonal subcell is shown dashed. After Jamieson *et al.* [2].

tungsten bronzes can be made in both single-crystal and ceramic forms, they have a myriad of applications in electronics [3].

## 1.2. Strontium barium niobate

In the mid-1960s, a group of ferroelectric niobates with the tungsten bronze structure was discovered, the members of which possess very useful electro-optic and non-linear optical properties [2]. These property characteristics make the niobates important in various ferroelectric devices, from heat sensors to electro-optic devices, which have varied civilian and military applications. Among these materials is strontium barium niobate (SBN), which has since proved to be one of the most useful members of this group because it has the largest electro-optic and pyroelectric coefficients in its class.

Fig. 6 shows the  $\text{SrNb}_2\text{O}_6$ – $\text{BaNb}_2\text{O}_6$  pseudobinary phase diagram [4]. Crystals of SBN can be grown from a melt of strontium niobate and barium niobate by the Czochralski method over the composition range from approximately 80% Sr: 20% Ba to 20% Sr: 80% Ba. The end members of the phase diagram,  $\text{SrNb}_2\text{O}_6$  and  $\text{BaNb}_2\text{O}_6$ , do not crystallize in a tungsten bronze structure. Instead,  $\text{BaNb}_2\text{O}_6$  crystallizes as either a hexagonal or orthorhombic structure, while  $\text{SrNb}_2\text{O}_6$  has a different orthorhombic structure which is isostructural with  $\text{CaTa}_2\text{O}_6$ . Therefore, interest in these materials lies within the solid solution region  $(\text{Sr}_{1-x}\text{Ba}_x)\text{Nb}_2\text{O}_6$ .

The structure for  $\text{Sr}_{0.75}\text{Ba}_{0.25}\text{Nb}_2\text{O}_6$  was solved over 20 years ago by Jamieson *et al.* [2]. It exhibits the space group  $P4bm$  with lattice parameters  $a, b = 1.243\ 024 \pm 0.000\ 002$  nm and  $c = 0.391\ 341 \pm 0.000\ 001$  nm. The theoretical density for the material is  $5.23$  g  $\text{cm}^{-3}$ .

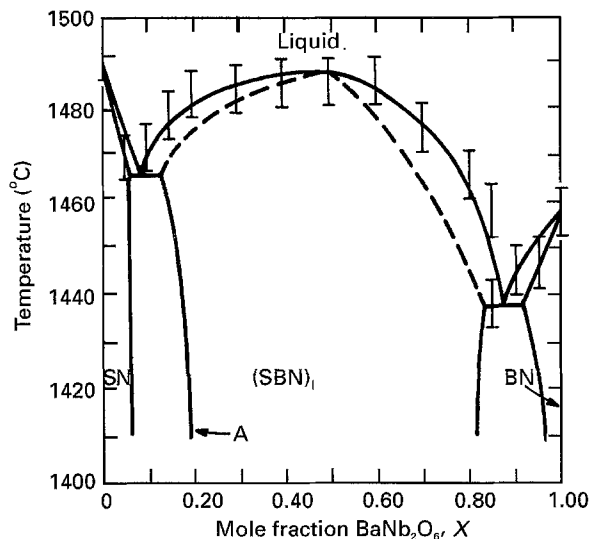


Figure 6 The pseudobinary phase diagram for the strontium niobate–barium niobate system. (–X)  $\text{SrNb}_2\text{O}_6$ – $X\text{BaNb}_2\text{O}_6$ , the solid solution; SN,  $\text{SrNb}_2\text{O}_6$  (ss); BN,  $\text{BaNb}_2\text{O}_6$  (ss); (– –) solidus. After Carruthers *et al.* [4].

Fig. 4 shows the distribution of the two A cations for the composition SBN(75–25) in the model proposed by Jamieson *et al.* [2]. Strontium and barium atoms share the A2 site in roughly a 1 to 3 ratio, while at the A1 site only strontium atoms are found. Neither site is fully occupied; the A1 site was found to have an 82% occupancy, while the A2 site, which the two cations share, has a total occupancy of 85%. The overall charge balance for the formula requires oxygen vacancies, which were considered to be at the O(4) site.

The structure devised by Jamieson *et al.* [2] is still accepted for SBN, although there has always been some question as to whether or not barium is found only on the A2 site. Positional disorder was investigated, but in the model with the best least-squares fit of calculated to experimental single-crystal X-ray diffraction data, barium was found only at the A2 site, and strontium occupies the A1 and A2 sites. A random distribution was not ruled out for other compositions of SBN or other thermal histories.

As the composition of SBN changes from  $x = 0.25$  to 0.52 Ba, the properties of the material change. The most notable change is that SBN shifts from a relaxor ferroelectric to a normal ferroelectric material. During this transition, the A1 sites become empty as the strontium content decreases. In addition, the  $a, b$  lattice parameters increase, possibly indicating that the  $\text{NbO}_6$  octahedra are shifting from a tilted to a more ordered (i.e. upright) arrangement. Finally, at a composition of  $x = 0.55$  Ba, the structure becomes orthorhombic [5], possibly due to a fundamental change in specific local structure sites, which in turn may be caused by the shifting of the  $\text{NbO}_6$  octahedra which leads to a global orthorhombic arrangement.

These changes suggest that, in the composition range  $x = 0.25$ –0.52 Ba, the local site symmetry is distorted because of the nature of the Sr/Ba atom placement in the A1 and A2 sites. The resulting Sr–Nb–Sr, Sr–Nb–Ba, and Ba–Nb–Ba interactions may be responsible for the incommensurate structure

found by Bursill and Peng [6]. These local structural distortions may, in turn, lead to changes in the polarization vectors due to shifts of the barium and strontium atoms between the oxygen sheets, causing the relaxor ferroelectric behaviour. When the amount of barium in the structure is increased beyond  $x = 0.52$ , and the  $\text{NbO}_6$  octahedra become more ordered, the polarization vectors no longer vary in magnitude and direction, and a shift to a regular ferroelectric material results.

### 1.3. The importance of disorder on material properties

Properties associated with the positional order-disorder phenomenon have been found in SBN. Glass [7] examined different compositions of  $\text{Sr}_{1-x}\text{Ba}_x\text{Nb}_2\text{O}_6$  and found that SBN took on the characteristics of a more ordered structure with increased percentage of barium in the material. Fig. 7 shows his plots of the dielectric constant at the transition temperatures for different compositions of SBN. The peaks for SBN with a composition of 73% Sr and 27% Ba (SBN(73–27)) are quite broad, while the peaks for SBN(48–52) are sharper, indicating that the cation order in SBN(48–52) is greater.

### 1.4. Objectives

The objectives of this work were to use X-ray powder diffraction and Rietveld structure refinement to investigate:

1. the trends in occupancy for strontium between the A1 and A2 site across the range of compositions for SBN(72–28) to SBN(50–50);
2. the possible occupancy of barium in the A1 site;
3. the shift in occupancy for strontium, in SBN(50–50), before and after the structure is annealed.

## 2. Experimental procedure

### 2.1. Source of strontium barium niobate

Single-crystal chips from boules of strontium barium niobate used for commercial devices for the three compositions, SBN(72–28), SBN(60–40), and SBN(50–50), were obtained from Dr Neurgaonkar, Rockwell International, Thousand Oaks, CA. These crystals were ground up for X-ray powder diffraction analysis.

### 2.2. X-ray fluorescence

X-ray fluorescence analysis was performed on the material SBN(72–28) using a Kevex  $\mu\text{x}$  System 0700. The material contained essentially the proper percentage by weight of strontium, barium, oxygen and niobium without the presence of any minor or trace elements. The values found were Nb  $47.34 \pm 0.95\%$ , Sr  $17.54 \pm 0.88\%$ , Ba  $10.14 \pm 0.10\%$ . The value for oxygen,  $24.77\%$ , was calculated by difference, because oxygen cannot be measured using X-ray fluorescence. The values calculated for the ideal composition of SBN (72–28) are O  $21.77\%$ , Nb  $50.58\%$ , Sr  $17.17\%$ ,

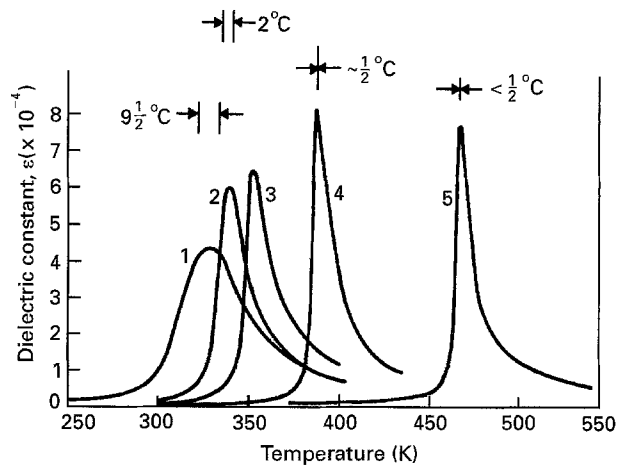


Figure 7 The dielectric constants of single-domain SBN crystals at 1 kHz as a function of material composition and temperature. Temperature transition ranges are shown above four of the dielectric peaks. After Glass [7]. Sample composition,  $\text{Sr}_{1-x}\text{Ba}_x\text{Nb}_2\text{O}_6$ , X: (1) 0.27, (2) 0.33, (3) 0.40, (4) 0.52, (5) 0.75.

Ba 10.47%. The strontium and barium compositions are both within  $\pm 0.40\%$  of the expected values, while niobium and oxygen are within about 3% of the expected values.

### 2.3. Sample preparation

The single-crystal chips of SBN(72–28), SBN(60–40), and SBN(50–50) in the unannealed state were initially ground to a powder using a ceramic mortar and pestle, and X-ray powder diffraction patterns were obtained. Rietveld refinement of these patterns resulted in a goodness of fit ( $R$ -value) of 17%–20% of the theoretical X-ray patterns generated by the program to the experimental patterns. A good  $R$ -value would be below 10%. It was suspected that the intensity measurements were in error. From the X-ray fluorescence analyses, these errors could not be due to impurities in the materials.

Megumi *et al.* [3] reported that grinding SBN crystallites to a diameter of approximately  $20 \mu\text{m}$  eliminated a similar problem in their X-ray diffraction patterns. Therefore, the SBN(72–28), SBN(60–40), and SBN(50–50) powders were wet ground in acetone using a  $\text{B}_4\text{C}$  mortar and pestle and then sieved dry using a 500 mesh screen ( $25 \mu\text{m}$ ). This method of grinding produced a particle size equal to or less than approximately  $25 \mu\text{m}$ . After reducing the average crystallite size to approximately  $25 \mu\text{m}$ , the Rietveld refinements yielded  $R$ -values of less than 10% for each SBN composition.

After the X-ray pattern for SBN (50–50) in the unannealed state was obtained, the material was placed in a platinum crucible and raised to  $550^\circ\text{C}$  over a period of 2 h at  $4.6^\circ\text{C min}^{-1}$ . The temperature was maintained at  $550^\circ\text{C}$  for 2 h; the sample was then furnace cooled very slowly from  $550^\circ\text{C}$  to room temperature over a period of approximately 20 h.

### 2.4. Density

The density of fragments of SBN(60–40) was measured using water displacement, and found to be

$5.41 \pm 0.04 \text{ g cm}^{-3}$ . The difference between the X-ray density of  $5.28 \text{ g cm}^{-3}$ , calculated from the Rietveld refined lattice parameters, and the measured density was  $0.13 \text{ g cm}^{-3}$ . The difference between the calculated X-ray density found for SBN(72–28) and the pycnometer density determined by Jamieson *et al.* was also  $0.13 \text{ g cm}^{-3}$ . Because the differences in both cases were relatively small, it was decided that precise pycnometer density measurements for each of the samples were not necessary.

SBN (75–25) has a X-ray density [2] of  $5.23 \text{ g cm}^{-3}$ , while the X-ray density of SBN(72–28) was  $5.24 \text{ g cm}^{-3}$ . The density for the two compositions differ by 0.19%. Therefore, the calculated X-ray densities could be used as a check against the models used for each composition.

## 2.5. X-ray pattern scans

A Philips APD 3600 automated X-ray powder diffractometer, with a  $2\theta$  compensating slit, and a Tektronix graphics terminal were used to collect the X-ray data. Copper radiation ( $\lambda = 0.15418 \text{ nm}$ ) was used, with a graphite monochromator, which deflected the beam a second time causing additional polarization. To correct for this polarization of the beam, a correction factor of 0.7897 was included in the input used for the Rietveld refinement calculations. The digitized data were corrected for the  $2\theta$  compensating slit [8] using the equation

$$I_{\text{corrected}} = I_{\text{observed}}/\sin \theta \quad (1)$$

The scan parameters were  $2\theta$  scan  $10^\circ$ – $130^\circ$ , step size  $0.01^\circ$ , count time 10 s.

## 2.6. Computer analyses

Data processing was done on a MicroVax II computer system (VMS). The Young and Wiles Rietveld structure refinement program [9] was used to determine the final occupancy values for the A1 and A2 sites.

The C site in the SBN structure is empty, but it is important in the discussion of possible changes in the surrounding A2 sites to know the coordination of this C site. The correct coordination for the C site was obtained by calculating bond distances and coordinations from single-crystal structure data for a material with a cation in this site,  $\text{K}_{6-x}\text{Li}_{4+x}\text{Nb}_{10+x}\text{O}_{30}$  [10], using the program DINT10 [11]. The calculated bond lengths for the coordinated oxygen atoms at the C site are listed in Table I. The results were checked with Pauling's radius ratio test. Shannon–Prewett ionic radii,  $\text{Li}^{+1} = 0.088 \text{ nm}$  and  $\text{O}^{-2} = 0.126 \text{ nm}$ , were used. The Li/O ratio is 0.698, and lithium is normally six-coordinated in oxygen compounds, but because the structure of SBN is distorted, a coordination value of nine is obtained.

## 3. Results

### 3.1. Final results for SBN

#### 3.1.1. Final structure refinement

Two starting models were used. In model 1, strontium is in the A1 site and strontium and barium share the

TABLE I Bond lengths calculated for the coordinated oxygen atoms from the fractional coordinates for  $\text{K}_{6-x}\text{Li}_{4+x}\text{Nb}_{10+x}\text{O}_{30}$  ( $X = 0.07$ ,  $Y = 0.23$ ) [5] at the C site

Atom 1	to	Atom 2	Distance (nm)
O(1)		Li(3)	0.25632
O(1)		Li(3)	0.23689
O(1)		Li(3)	0.25632
O(1)		Li(3)	0.23689
O(3)		Li(3)	0.26030
O(3)		Li(3)	0.24809
O(4)		Li(3)	0.20909
O(5)		Li(3)	0.21650
O(5)		Li(3)	0.21650

Lattice parameters:  $a$ ,  $b = 1.25066 \text{ nm}$ ,  $c = 0.391640 \text{ nm}$ .

A2 site. For this model, only the values for the strontium occupancies were varied for the two sites, with barium constrained to the A2 site. In model 2, 5% of the barium atoms are placed at the A1 site so that it shares occupancy there with strontium atoms, and strontium and barium share the A2 site. The barium and strontium occupancies for both the A1 and A2 sites were refined. The results of the refinements of the models, both of which give reasonable structures for SBN, are listed in Table II.

#### 3.1.2. $R_p$ values (per cent goodness of fit)

The final  $R_p$  values for models 1 and 2 for SBN(72–28) were both 9.8%. The  $R_p$ s were high because the (001) and (002) reflections were relatively larger than the calculated peaks for this material (see Figs 8 and 9). The small (620) peak adjacent to the (002) reflection had a calculated intensity larger than the observed value, indicating that the difference between the calculated and observed (100) and (200) peaks was due to some factor other than an error in scaling the observed to the calculated patterns. The final refinements were carried out with no correction for preferred orientation; when a preferred orientation correction was included, considerably higher  $R_p$  values resulted.

For SBN(60–40), the final  $R_p$  value was 7.76% for both models.

The final  $R_p$  values for SBN(50–50) in the unannealed and annealed states for model 1 were 8.72% and 8.03%, respectively. These values are acceptable for a structure as disordered as strontium barium niobate.

#### 3.1.3. Refinement results for SBN

The final structure refinements for the three unannealed samples indicated that there are essentially no barium atoms in the A1 site. When an attempt was made to place barium atoms in the A1 site for SBN(72–28) (model 2), the occupancy value for this site decreased to near zero. The refined structure for model 2 for SBN(60–40) had an apparent final A1 occupancy value for barium of 4%. This appears to be an aberrant result because the refinements for the

TABLE II Refined values for the final models of SBN

Composition	Model	$R_p$ factor	Site	Cation	Partial occupancy (%)	Total occupancy of site (%)
SBN (72-28), unannealed	1	9.82%	A1	Sr		$70.28 \pm 0.0006$
			A2	Sr	54.10	
			A2	Ba	36.56	
			A2	Sr/Ba		
	2	9.82%	A1	Sr		68.12
			A1	Ba	1.48	
			A1	Sr/Ba		
			A2	Sr	54.10	
			A2	Ba	35.82	
			A2	Sr/Ba		
SBN (60-40), unannealed	1	7.76%	A1	Sr		$64.64 \pm 0.0006$
			A2	Sr	41.98	
			A2	Ba	51.50	
			A2	Sr/Ba		
	2	7.76%	A1	Sr	58.48	62.64
			A1	Ba	4.16	
			A1	Sr/Ba		
			A2	Sr	49.42	
			A2	Ba	45.06	
			A2	Sr/Ba		
SBN (50-50) unannealed	1	8.72%	A1	Sr		$54.08 \pm 0.0007$
			A2	Sr	36.50	
			A2	Ba	62.26	
			A2	Sr/Ba		
SBN (50-50)	1	8.03%	A1	Sr		$61.88 \pm 0.0006$
			A2	Sr	32.60	
			A2	Ba	62.26	
			A2	Sr/Ba		

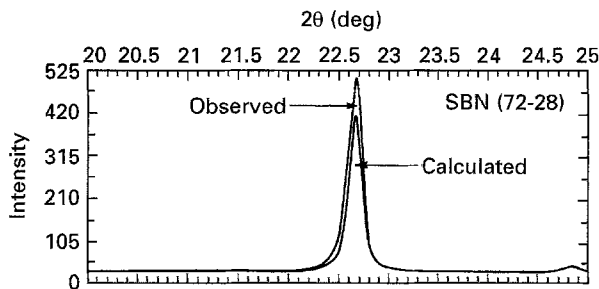


Figure 8 The observed and calculated (001) peak profiles.

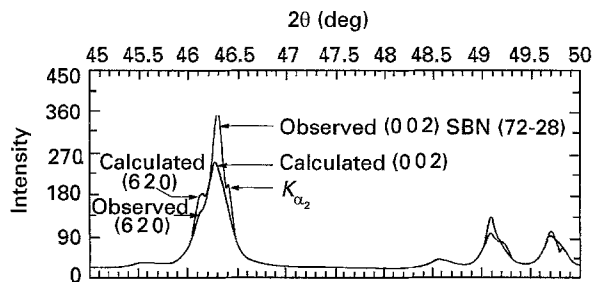


Figure 9 The observed and calculated (002) peak profiles. The second peak overlapped with the (002) reflection is the (620) reflection.

other compositions all indicated that, if there is room for barium in the A2 sites, then no barium will occupy the A1 sites. For example, model 1 for unannealed SBN(50-50) indicated that barium cannot occupy the A1 site because, in this case, only the strontium occu-

pancies were varied, and the refinement showed that the A2 site was essentially completely occupied by barium and strontium. The placement of 5% Ba on the A1 site would have forced the A2 occupancy to increase to over 100% which is physically impossible. Therefore, to obtain a refinement in which the occupancies were 100% or less, only strontium could be placed in the A1 site.

The cation distribution in the three unannealed materials is quite significant. The strontium atoms show a preference for the A1 site by a roughly constant factor of about 1.5. When barium is substituted for strontium, the strontium occupancies of the A1 and A2 sites decrease proportionally by about the same amount, but the larger barium ions only occupy the larger A2 sites.

Annealing apparently allows strontium atoms to move from the A2 site to the A1 site. Upon annealing the SBN(50-50) material, the strontium occupancy in the A1 site increased significantly from 54% to almost 62%.

## 4. Discussion

### 4.1. Comments on the refinement procedure

A large variety of structure refinement procedures for strontium barium niobate were tried. For the final structure refinements, all the background parameters, lattice parameters and occupancy values for the A1 and A2 sites were varied. Initial isotropic temperature factors,  $B$ , and  $X$ ,  $Y$  and  $Z$  coordinates from the structure of Jamieson *et al.* [2] were not varied. The

decision to restrain  $X$ ,  $Y$ ,  $Z$  and  $B$  was made after attempts to refine them failed to converge. The final  $R$ s were significantly lower for the partial structure refinements than for the full structure refinements.

When a refinement converges, it reaches a final  $R$  value, and the parameters being varied no longer change. This final  $R$  is not necessarily the global minimum, but corresponds to the best fit to the pattern, given the set of parameters being refined and the observed data. The  $R$ s for refinements that did not converge either oscillated with each cycle or increased

in value. Fig. 10 gives the order in which each factor was refined for each of the compositions.

The occupancies can be refined without the other structure parameters because  $X$ ,  $Y$ ,  $Z$  and  $B$  values do not change significantly from one composition to another. In the tetragonal tungsten bronze structure, Nb(1) and the A(1) cation at the A1 site always occupy the equipoints  $2b$  and  $2a$ , respectively. The  $2a$  and  $2b$  sites have fixed  $X$  and  $Y$  coordinates. The coordinates for the  $2a$  site are  $(0\ 0\ Z)$  and  $(\frac{1}{2}\ \frac{1}{2}\ Z)$  and for the  $2b$  site  $(\frac{1}{2}\ 0\ Z)$  and  $(0\ \frac{1}{2}\ Z)$  [12]. There are only a limited

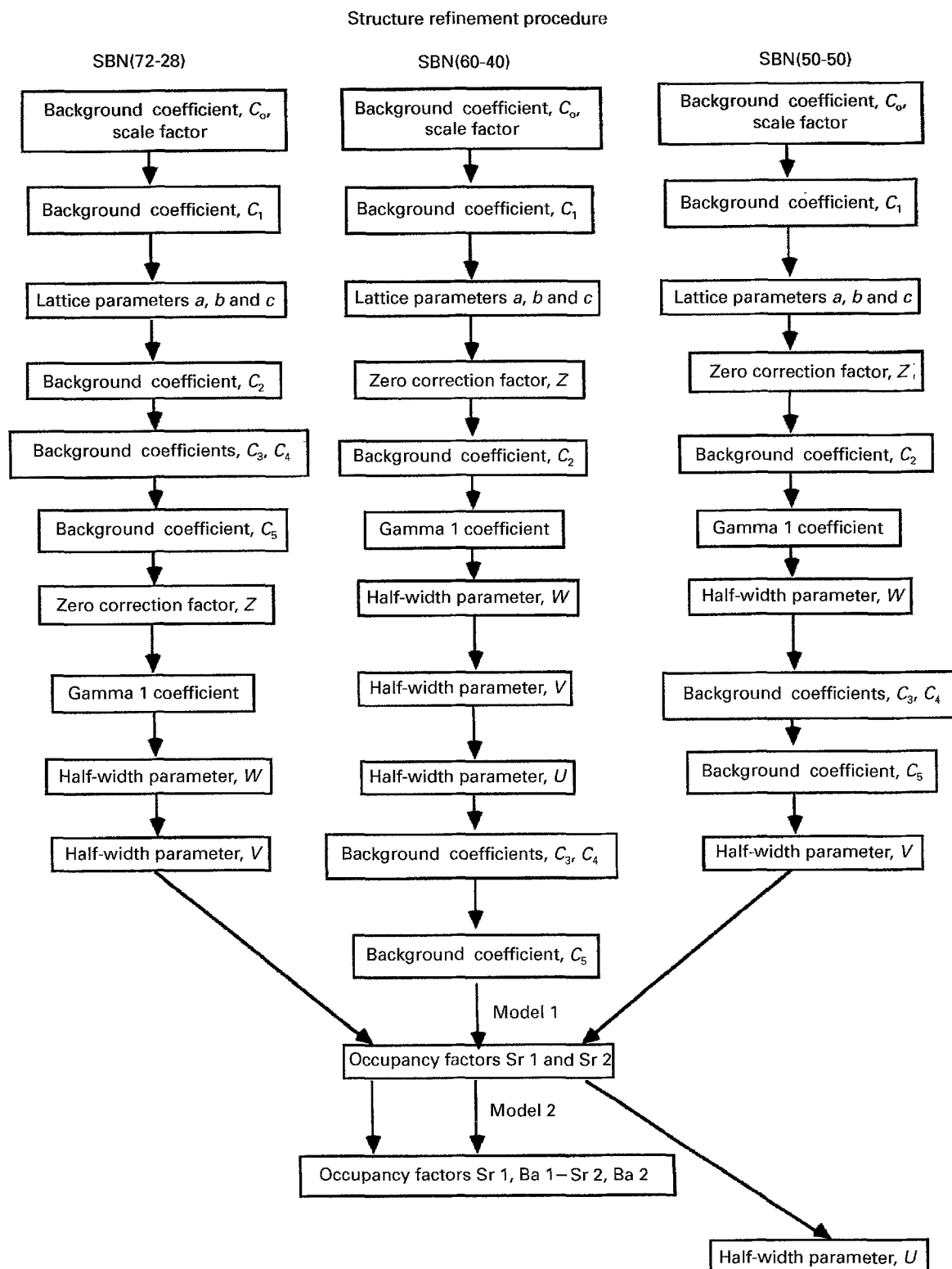


Figure 10 A flow chart of the order in which each of the parameters was refined during structure refinement for each composition of SBN.

number of ways in which the atoms surrounding those in the 4*c* and 8*d* sites can be arranged and still maintain the *P4bm* symmetry. These constraints on atomic positions permit the *X*, *Y* and *Z* values to be fixed during refinement.

The same reasoning holds for the isotropic temperature factors. There is little significant difference in the isotropic temperature factors from one composition to another. For the atoms to have very different isotropic temperature factors, a substantial change in the structure of the material would be necessary. Again, the results from converged and non-converged refinements dictated restraint of these structure parameters.

Bond distances were another indication that attempting to refine *X*, *Y*, *Z* and *B* values simultaneously with the other parameters was not correct. When *X*, *Y*, *Z* and *B* were varied, some of the resulting bond lengths were outside acceptable values.

Finally, the correlation matrix showed that the atomic coordinates and isotropic temperature factors were highly correlated with other refinement parameters. All parameters could not be refined simultaneously perhaps because the information is masked by the domain structure within the material [6].

#### 4.2. A1 and A2 occupancies

The A2 site in the SBN structure has traditionally been considered smaller than the A1 site because the coordination of the A1 site is twelve and the A2 site is nine coordinated. The A2 site should have shorter bond lengths and a smaller volume than the A1 site. This assumption that the A1 site is larger than the A2 site in the tungsten bronze structures appears to be incorrect. When the local site symmetry is not distorted, the twelve coordinated site should be larger than the nine coordinated site. In SBN(75–25), the local site symmetry is distorted: “... the A1 site has 12 nearest oxygen atoms in distorted cubo-octahedral coordination” and “... the A2 site may be described as a distorted tri-capped trigonal prismatic coordination...” [2].

To determine if the A1 site is larger or smaller than the A2 site, bond lengths were calculated for the struc-

ture of SBN(75–25), using the program DINT10 [11] and the *X*, *Y* and *Z* coordinates of Jamieson *et al.* [2]. The average length for the O–Sr bonds at the A1 site was found to be shorter than the average length for the O–Sr/Ba bonds at the A2 site. Table III contains the results of these average bond-length calculations. It is clear, then, that there is more room for the cations at the A2 site. Therefore, if the A1 site became too small for even strontium to occupy, due to structural distortions, strontium would then locate in the larger A2 site. These differences in size also explain why cations larger than strontium locate at the A2 site; no barium could be found at the A1 site.

The A1 site in the unannealed state is most likely smaller than in the annealed state of SBN. The unannealed samples of SBN(72–28), SBN(60–40), and SBN(50–50) were all from crystalline material taken directly from a boule grown from a melt. In the unannealed state, the coordinations of the A1, A2 and C sites are distorted by a twisting of the sheet structure, leaving the cages with less volume to accommodate the cations. Small changes observed in the lattice parameters of SBN(50–50) upon annealing support this idea. In the unannealed state,  $a, b = 1.24739 \pm 0.00002$  nm and  $c = 0.39506 \pm 0.00001$  nm, while in the annealed state  $a, b = 1.24746 \pm 0.00002$  nm, and  $c = 0.39488 \pm 0.00001$  nm. The  $a, b$  lattice parameters for the annealed material are longer by 0.00007 nm and the  $c$  parameter is shorter by 0.00018 nm. The larger values for the  $a, b$  parameters and smaller  $c$  parameter for SBN(50–50) in the annealed state indicate that the structure flattens out, becoming somewhat more regular and less twisted.

Also, because the C site is tri-capped trigonal prismatic, with O(4) and O(5) atoms between the A1, A2, and C sites, the M(1) and M(2) octahedra can shift between more than the two positions originally devised for the O(4) and O(5) atoms [2]. With greater latitude of motion for these oxygen atoms, the octahedra, rather than just tilting back and forth in one direction, can tilt in many directions, creating more ways for the structure to distort than previously expected. This additional distortion could account for the reduction in size of the A1, A2 and C cages when

TABLE III Average bond-length calculations for sites A1 and A2 using values taken from Jamieson *et al.* [2]

Site	Coordination	Atom 1	Atom 2	Distance (nm)	No. of Bonds
A1 cubo-octahedral coordination	12 oxygens about the Sr atom	Sr(1)	O(2)	$0.2547 \pm 0.0008$	4
		Sr(1)	O(2)	$0.2919 \pm 0.0008$	4
		Sr(1)	O(5A)	$0.267 \pm 0.0020$	2
		Sr(1)	O(5B)	$0.285 \pm 0.0020$	2
A2 tricapped trigonal prismatic coordination	9 oxygens about the Sr/Ba atoms	Ba/Sr	O(1)	$0.3035 \pm 0.0010$	2
		Ba/Sr	O(1)	$0.2707 \pm 0.0010$	2
		Ba/Sr	O(3)	$0.2844 \pm 0.0009$	1
		Ba/Sr	O(3)	$0.2604 \pm 0.0009$	1
		Ba/Sr	O(4)	$0.2758 \pm 0.0009$	1
		Ba/Sr	O(5A)	$0.287 \pm 0.0020$	2

$$\text{Average bond length for A1 site} = \frac{3.2904 \pm 0.0144 \text{ nm}}{12 \text{ atoms}} = 0.275 \pm 0.0012 \text{ nm.}$$

$$\text{Average bond length for A2 site} = \frac{2.543 \pm 0.0107 \text{ nm}}{9 \text{ atoms}} = 0.2826 \pm 0.0012 \text{ nm.}$$

$$\text{Difference between the average bond lengths} = 0.2826 \pm 0.0012 \text{ nm} - 0.275 \pm 0.0012 = 0.0084 \pm 0.0012 \text{ nm.}$$

the crystal is first grown and lead to the preference of the strontium for the larger A2 site.

The situation is different for the SBN(75–25) material studied by Jamieson *et al.* [2], which was continuously poled “by application of a  $150 \text{ V cm}^{-1}$  field along the *c* axis at 388 K followed by slow cooling in the electric field”. It is suggested here that the structure of this material may be less distorted than the structure of SBN(72–28) in the sense that the sheets of oxygen octahedra are flatter. It is further suggested again that the flattening of these sheets in some way may enlarge the A1 cage so that it can more easily accommodate the cations. In fact, the occupancy value for the A1 site in SBN(75–25) was over 12% higher than that for the A1 site in SBN(72–28). A similar increase in strontium occupancy of the A1 site was observed in the present study in SBN(50–50) upon annealing (see Table II).

The changes in the structure of SBN(72–28), SBN(60–40) and SBN(50–50) coincide with changes in composition. For example, the dielectric peak (Fig. 7) shifts from a diffuse peak at SBN(72–28) to a sharp peak at SBN(50–50). Also, other properties shift from those of a ferroelectric relaxor to a normal ferroelectric [4] as the composition shifts to a higher percentage of barium atoms. Because barium atoms were not found at the A1 site, random cation disorder cannot account for these property shifts, as proposed by Setter [13]. Therefore, it is probable that the distortion of the structure accounts in part or in whole for the shift in the material properties.

## 5. Conclusion

From Rietveld refinements of powder X-ray diffraction data for unannealed SBN(72–28), SBN(60–40), and SBN(50–50) and annealed SBN(50–50), it was found that (1) there is no barium on the A1 site in the structure, (2) both barium and strontium prefer to locate at the A2 site in the unannealed materials, and (3) on annealing, some of the strontium atoms migrate to the smaller A1 sites.

The positions of the cations in the structure appear to be due to a twisting of the structure in its unan-

nealed state. In the unannealed material, the twisted structure reduces the size of the A cation cages. This twisting makes it difficult for strontium cations to locate at the A1 site. Hence, the strontium cations locate at the larger A2 site. When the material is annealed, the structure flattens out, enlarging the A1 and A2 sites, reducing the distortion of the overall structure of the material, and allowing the smaller strontium cation to migrate to the smaller A1 site. The shift in the properties of these materials appears to be linked to the distortion of the structure.

## Acknowledgement

One of the authors (M.P.T.) acknowledges the support of Rockwell International Corporation in this research.

## References

1. A. MAGNELI, *Ark. Kemi.* **1** (1949) 213.
2. P. B. JAMIESON, S. C. ABRAHAMS and J. L. BERNSTEIN, *J. Chem. Phys.* **48** (1968) 4352.
3. K. MEGUMI, N. NAGATSUMA, Y. KASHIWADA and Y. FURUHATA, *J. Mater. Sci.* **11** (1976) 1583.
4. J. R. CARRUTHERS and M. GRASSO, *J. Electrochem. Soc.* **117** (1970) 1426.
5. I. G. ISMAILZADE, *Kristallogr.* **5** (1960) 268.
6. L. A. BURSILL and J. L. PENG, *Philos. Mag.* **B54**(2) (1986) 157.
7. A. M. GLASS, *J. Appl. Phys.* **40** (1969) 4699.
8. A. L. DRAGOO, *J. Powd. Diff.* **1** (1986) 294.
9. R. A. YOUNG and D. B. WILES, National Bureau of Standards Special Publication 567 (National Bureau of Standards, Washington, DC, 1980) pp. 143–62.
10. S. C. ABRAHAMS, P. B. JAMIESON and J. L. BERNSTEIN, *J. Chem. Phys.* **54** (1971) 2355.
11. D. K. SMITH, *J. Appl. Crystallogr.* **24** (1991) 369.
12. T. HAHN (Ed.), “International Tables for Crystallography”, Vol. A, Reidel, Dordrecht, Boston, Lancaster, Tokyo, 1987).
13. N. SETTER, PhD thesis, The Pennsylvania State University (1980).

*Received 4 January*

*and accepted 8 September 1995*